Experimental Verification of 3D Eddy Current Analysis Code Using T-method

doi: 10.1109/20.106356

EXPERIMENTAL VERIFICATION OF 3D EDDY CURRENT ANALYSIS CODE USING T-METHOD

Toshiyuki Takagi, Mitsuo Hashimoto, Seiji Arita,
So Norimatsu, Toshihiko Sugiura, Kenzo Miya
Nuclear Engineering Research Laboratory,
The Faculty of Engineering, The University of Tokyo,
Tokai, Ibaraki 319-11, Japan

Abstract

This paper describes an experimental verification of a 3D eddy current analysis code based on T-method by applying it to an eddy current testing(ECT) problem. ECT experiments were carried out for a standard problem proposed by the TEAM Workshops. Numerical results agreed with experimental ones in some important features. This shows the validity of the method and the code for 3D eddy current problems.

Introduction

There are many approaches to 3D eddy current analysis. Typical methods for the eddy current analysis are the A-ϕ method and the T-Ω method. Both methods require variables in space as well as in a conductor. We have already proposed the T-method [1, 2, 3, 4], where a magnetic scalar potential Ω of T- Ω method is not included. Advantages of the T-method are : (1)only one variable (one vector with three components), (2)no variables in space and (3)easy treatment of external current and field.

But the method has a disadvantage that a large core memory is needed due to a dense matrix. In order to overcome this difficulties, we have proposed an iterative solution technique for the T-method. The preliminary results have been presented [3].

TEAM(Testing Electromagnetics Analysis Method) Workshops [5, 6, 7, 8, 9] are now under way. The ultimate goal of the TEAM Workshops is to compare the numerical results solved by many computer codes, to verify the modellings, numerical techniques and computer codes, and to gain confidence in their predictions [6]. One of the TEAM Workshop problems is an ECT(eddy current testing) problem.

The ECT is a type of non-destructive testing and effective for detecting surface cracks or flaws in conductive materials. Since this phenomenon is 3D in nature, 3D numerical analysis is required in order to know eddy current distribution in the conductor and to improve the ECT technique. We have already applied the T-method to an ECT problem (TEAM problem No.8) [3, 4]. But the results were not in good agreement with experimental values. Therefore in this study we repeated the experiment and improved the way of analysis. One reason for the difficulties of the ECT analysis is that we usually use the differential probe and need very high accuracy in calculating magnetic field. Another reason is that it is not easy to treat the applied field caused by an external active probe coil when we use an eddy current analysis method which needs mesh division in space. But it is now well understood that the numerical analysis plays a very important role for the solution of both forward and inverse ECT problems [10].

The purposes of this paper are : (1) development of practical eddy current analysis method using T-method, (2) measurement of signal trajectories for an ECT of a block with a flaw (TEAM problem No.8) and (3) application of the method to this ECT problem and the verification of the method.

Eddy Current Analysis

In this section we show the derivation of the governing equations of the T-method, and an iterative solution technique and the developed computer code are described.

Basic Equations

The following two of four Maxwell equations are enough to determine transient distribution of eddy current.

$$\nabla \times \vec{H} = \vec{J} \quad and \quad \nabla \times \vec{E} = -\left(\frac{\partial \vec{B}_e}{\partial t} + \frac{\partial \vec{B}_o}{\partial t}\right) \tag{1}$$

where $\vec{H}$ and $\vec{J}$ are magnetic field and current density vectors. $\vec{B}_e$ and $\vec{B}_o$ are induced and applied magnetic induction vectors. $\vec{B}_o$ can be calculated directly using Biot-Savart's law. These equations are supplemented with the following constitutive equations.

$$\vec{B} = \mu_o \vec{H} \quad and \quad \vec{J} = \sigma \vec{E} \tag{2}$$

where μ_o and σ are magnetic permeability of air and electrical conductivity. Since displacement current is neglected in eq.(1), the conservation of current is secured. Thus current vector potential, T, is defined as,

$$\vec{J} = \nabla \times \vec{T}. \tag{3}$$

Biot-Savart's law is written as,

$$\vec{B}_e = \frac{\mu_o}{4\pi} \int_v \vec{J}' \times \nabla' \frac{1}{R} dV'. \tag{4}$$

After mathematical manipulation and calculation the relation between the induced magnetic induction and the current vector potential is given as the following equation [1].

$$\vec{B}_e = \mu_o \vec{T} + \frac{\mu_o}{4\pi} \int_s T_n' \nabla' \frac{1}{R} dS' \tag{5}$$

Governing Equations of T-Method

Introducing eq.(5) into eq.(1) and using eq.(3), we obtain the governing equation for the eddy current analysis.

$$\nabla \times \frac{1}{\sigma} \nabla \times \vec{T} + \mu_o \frac{\partial \vec{T}}{\partial t} + \frac{\mu_o}{4\pi} \int_s \frac{\partial T_n'}{\partial t} \nabla' \frac{1}{R} dS' + \frac{\partial \vec{B}_o}{\partial t} = \vec{0} \tag{6}$$

In this paper we deal with an AC problem. Eq.(6) is rewritten for sinusoidal field using imaginary unit, j, and angular frequency, ω.

$$\nabla \times \frac{1}{\sigma} \nabla \times \vec{T} + j\omega\mu_o \vec{T} + j\omega \frac{\mu_o}{4\pi} \int_s T_n' \nabla' \frac{1}{R} dS' + j\omega \vec{B}_o = \vec{0} \tag{7}$$

We solve eq.(7) with the following gauge condition and boundary condition on conductor surface using the finite element method.

$$\nabla \cdot \vec{T} = 0 \quad and \quad \vec{T} \times \vec{n} = \vec{0} \tag{8}$$

Matrix Equation Using Iterative Solution Technique

The Galerkin method using second-order 20 nodes isoparametric elements is applied to solve eq.(7). The obtained coefficient matrix is complex, unsymmetric and dense. A direct matrix equation solution procedure such as Cholesky decomposition method

0018-9464/90/0300-0474$01.00 © 1990 IEEE

has been used. In this iteration technique, we split the matrix into two matrices. One matrix corresponds to the first and second terms of eq.(7). It is a complex, symmetric band matrix. The other corresponds to the third term, *"non-local term"*. It is imaginary, unsymmetric and almost dense.

The iterative method is proposed where the current vector potential in the n-th iteration can be obtained as the solution of the following equation.

$$[P]\left\{T^{(n)}\right\} = \left\{f^{(n)}\right\} \tag{9}$$

where

$$\left\{f^{(n)}\right\} = \alpha\left[\{B_o\} - [Q]\left\{T^{(n-1)}\right\}\right] + (1-\alpha)\left\{f^{(n-1)}\right\} \tag{10}$$

α : relaxation factor
(n) : n-th iteration
$[P]$: Complex, symmetric, band matrix
$[Q]$: Imaginary, unsymmetric, dense matrix

Computer Code

The computer code "ELMES" was developed based on the T-method described above. Fig.1 shows the calculation flow of the code. After data are input, coefficient matrices are generated and the right-hand side vector, which corresponds to external field, is calculated. Then using the iterative technique the distribution of the current vector potential is obtained. Finally we get magnetic field distribution from the potential.

Experiment

As an ECT problem, we adopted the standard one proposed in the TEAM Workshops for eddy current code comparison [5] and also presented in some papers [11, 12]. The test piece is a rectangular block 330x285x30mm with a 40x0.5x10mm flaw on the center of one of the larger faces, as shown in Fig.2. It is made of austenitic steel type 18-10 Mo with less than 2% of ferrite. Relative permeability μ_r is 1 and electrical conductivity σ is $0.14 \times 10^7 S/m$.

A differential probe (Fig.3) moves on the surface of the block. The probe is a cylinder with an active solenoid and two smaller receptive solenoids. The block diagram of an ECT device used here is shown in Fig.4. An oscillator supplies sine wave into the active solenoids. We obtain the exact phase angle which we can compare with that obtained in the numerical analysis. By moving the probe, we obtain signal trajectory which corresponds to the image, on the complex plane, of the difference of magnetic fluxes through the two receptive solenoids. The experiments were carried out for 2 different movements of the probe (parallel and perpendicular to the flaw) under 2 different frequencies(500Hz, 1kHz).

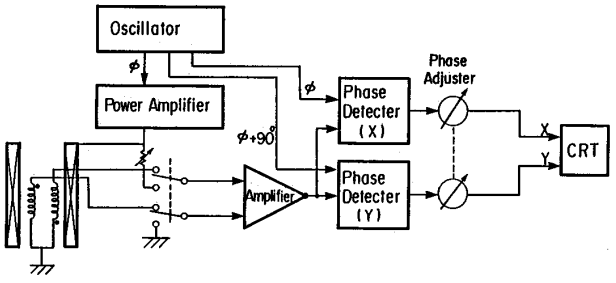

Fig.4 Block diagram of ECT device

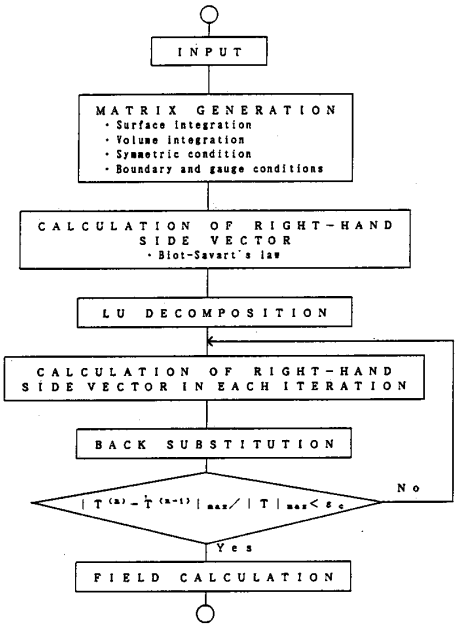

Fig.1 Flow of eddy current analysis

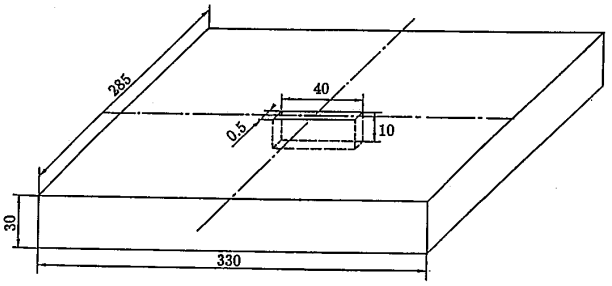

conductivity : $\sigma = 1.4\times10^6\ s/m$
relative permeability : $\mu_r = 1$
frequency : $f = 500Hz$

Fig.2 The Block with a flaw as ECT model

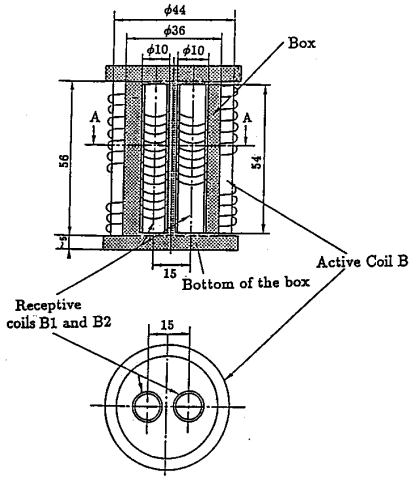

Fig.3 Configuration of the probe

Results and Discussions

In Figs. 5(a),6(a),7(a), and 8(a) are shown experimental results for coil motion parallel and perpendicular to the flaw. The results show symmetric trajectories about the zero point. Phase angle changes as the frequency changes.

Numerical analysis was also carried out for the same problem. For the symmetry the region to be meshed is only a half of the block. The flaw is treated as a low conductive region and included in the analysis domain. The conductivity was assumed $5.0 \times 10^2 S/m$, which is low enough compared to that of the block. Fig.9 shows examples of mesh division when the coil moves parallel to the flaw. Table 1 gives the number of nodes, elements, unknowns, and CPU time. We used a supercomputer HITAC S-820 made by Hitachi, Ltd. CPU time was 4-6 minutes and needed memory was 108 MBytes.

Fig.10 shows the eddy current distribution on the top surface when the coil locates at x=80 mm. One can see that eddy current concentrates locally near the coil and current is very small at a location more than 100 mm distant from the coil. This fact gives us an idea that region near the coil should be divided into fine meshes though far region need not be. Therefore, according to each coil position, we used a different type of mesh division in the x direction (Fig.11). In order to get high accuracy of magnetic field calculation much attention was paid for the symmetric mesh division in the region near the coil.

In each coil location the flux of the induced field is calculated through the two receptive solenoids and the difference between them gives a point of the output signal. After the calculation at all coil locations, connecting these signal points indicates the signal trajectory. Figs.5, 6, 7 and 8 show the comparison of the numerical and experimental results for a coil movement parallel and perpendicular to the flaw when the frequency is 500Hz and 1kHz. Results show almost good agreement both in shape and phase angle. Phase angle changes as the frequency changes both in analysis and experiment in the same manner.

One reason for the discrepancy may be the lack of accuracy in both the numerical simulation and the experiment. The output signal here is the difference of fluxes through the two solenoids which are very close to each other. For example when the coil moves parallel to the flaw and the coil location was x=-10mm, the calculated magnetic flux (in complex number) of two solenoids were (3.2256×10^{-12}, 2.2828×10^{-12}) and (3.2084×10^{-12}, 2.2663×10^{-12}). Therefore the difference of two coils fluxes is (1.7166×10^{-14}, 1.6494×10^{-14}). From the numerical point of view, it requires higher accuracy, compared with current vector potential itself. And the number of meshes, especially for the region near the coil, may not yet be enough to achieve the very high accuracy. From the experimental side, there are some deficiencies in the electrical specification of the coil so that there may be a low sensitivity problem especially when the frequency is low.

The following "*Zooming*" technique may be applicable in order to get higher accuracy in 3D eddy current problems.

"Zooming" Fig.12 shows the distribution of normal component of current vector potential with and without the flaw (coil location (y=-10mm), f=500Hz, perpendicular). Values of current vector potential with the flaw agreed with the values without the flaw except the region near the coil and the flaw. This means that we can analyze only the important region using the values of rough calculation with fewer elements as the boundary condition.

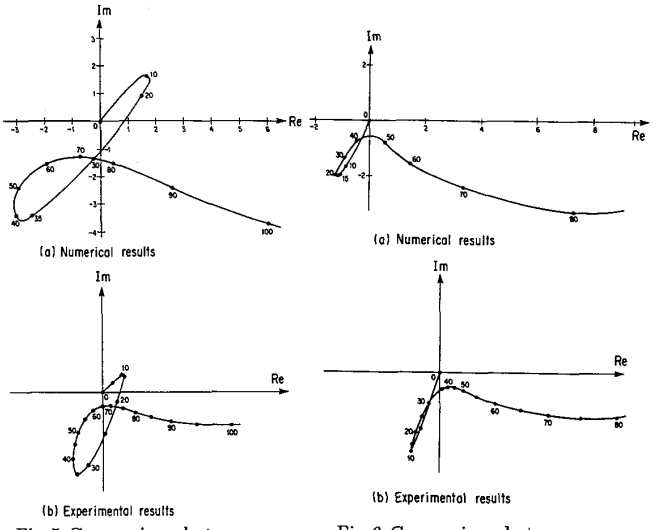

Fig.5 Comparison between numerical and experimental results (f=500Hz, coil motion parallel to a flaw)

Fig.6 Comparison between numerical and experimental results (f=500Hz, coil motion parallel to a flaw)

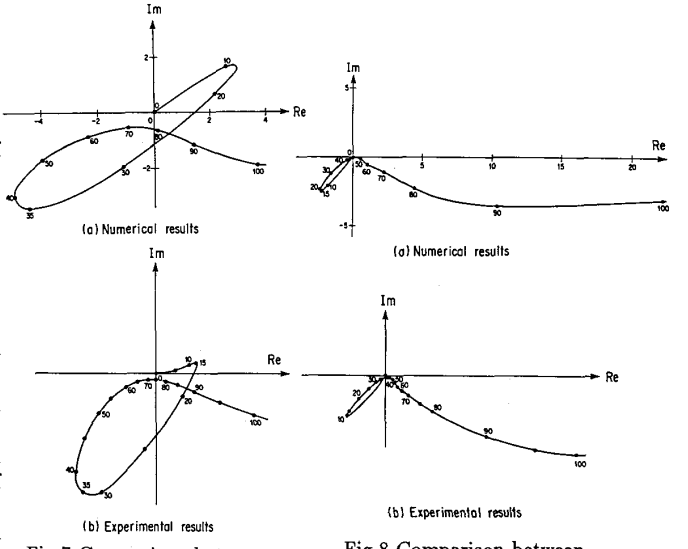

Fig.7 Comparison between numerical and experimental results (f=1kHz, coil motion parallel to a flaw)

Fig.8 Comparison between numerical and experimental results (f=1kHz, coil motion perpendicular to a flaw)

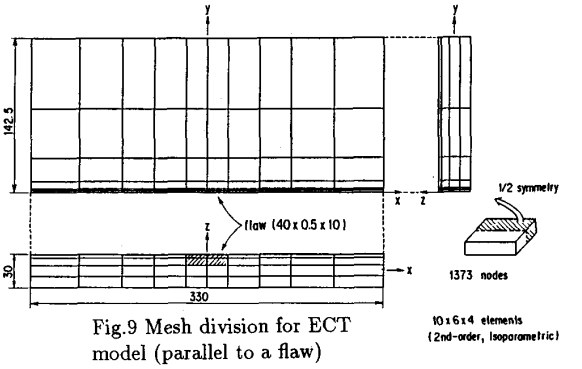

Fig.9 Mesh division for ECT model (parallel to a flaw)

Conclusions

1. A numerical technique of 3D eddy current analysis and a computer code "ELMES" was developed.
   (a)Current vector potential (T) method with iterative solution technique was successfully developed.
   (b)Mesh division was adapted to the position of coils and a flaw.

2. Signal trajectories for ECT of a block with a flaw were measured.
   (a)Experiment was performed for a benchmark problem of TEAM Workshops under two frequencies (500Hz and 1kHz).

3. The method was applied to this ECT problem.
   (a)Numerical results for 500Hz and 1kHz agreed with measured values in almost good accuracy.
   (b)In order to get higher accuracy. A "*Zooming*" technique may be applicable to 3D calculation.

References

[1] K.Miya et.al.,"Three Dimensional Analysis of Eddy Current by the T-Method", Proceedings of the IUTAM Symposium, Tokyo, October, North-Holland, 1986, pp.183-189.

[2] K. Miya and H. Hashizume, "Application of T-method to AC Problem Based on Boundary Element Method," IEEE Transactions on Magnetics, Vol.24, January, 1988, pp.134-137.

[3] T.Takagi et. al.,"Iteration Solution Technique for 3-D Eddy Current Analysis Using T-Method, "IEEE Transactions on Magnetics, Vol.24, No.6, November, 1988, pp.2682-2684.

[4] T. Sugiura, et al., "Numerical Analysis of Non-Destructive Testing with a 3-D Eddy Current Code "ELMES" Based on T-method," BISEF Conf., Beijing, December, 1988.

[5] L.R. Turner, "TEAM Test Problems", ANL, April 1988.

[6] L.R. Turner et al., "Workshops and Problems for Benchmarking Eddy Current Codes," ANL/FPP/TM-24.

[7] L.R. Turner, "Proceedings of the Vancouver TEAM Workshop at the University of British Columbia 18 and 19 July 1988," ANL/FPP/TM-230.

[8] J.C. Verite et. al., "TEAM Workshop and Meeting on the Applications of Eddy-Currents Computations," Meeting Proceedings, Bievres, France, March 20-22, 1989.

[9] N. Ida, "Proceedings of the Baltimore TEAM Workshop at the Johns Hopkins University 3 and 4 of April 1989," The Univ. of Akron, 1989.

[10] W. Lord, "Development in the Numerical Modeling of NDT Phenomena," Applied Electromagnetics in Materials, Pergamon Press, 1989, pp.117-125.

[11] J.C. Verite, "Application of a 3-D Eddy Current Code (TRIFOU) to Non-Destructive Testing," COMPEL, Vol.13, 1984, pp.167-178.

[12] A. Bossavit and J.C. Verite, "The TRIFOU" Code: Solving the 3-D Eddy Currents Problems by Using H as State Variable," IEEE Transactions on Magnetics, Vol.19, November 1983, pp.2465-2470.

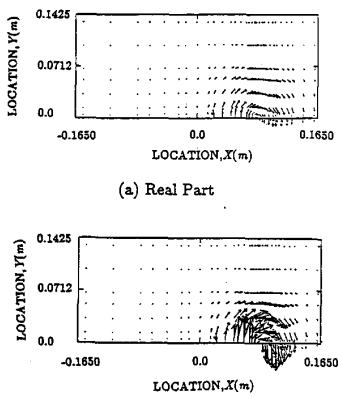

Fig.10 Eddy current distribution on top surface (coil:x = 80mm, y = 0mm)

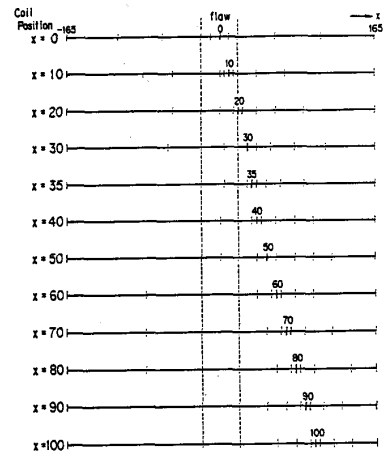

Fig.11 Mesh division in the x direction adapted to each coil position (parallel to a flaw)

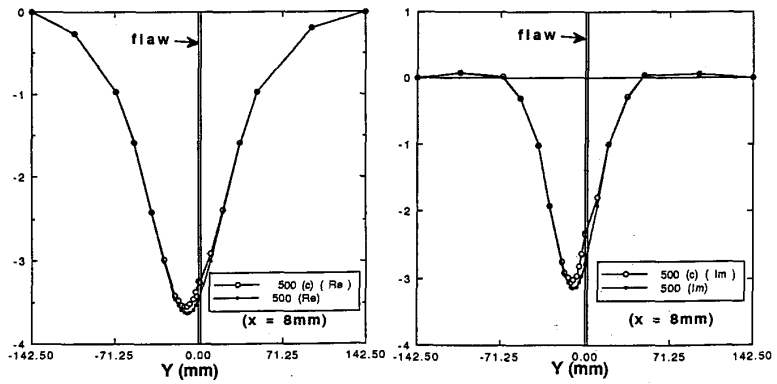

Fig.12 Distribution of normal component of current vector potential with (symbol of "o ") and without a flaw(symbol of "•") (coil location:y=-10mm, f=500Hz,perpendicular)

Table 1 Number of nodes, elements, unknowns and CPU time (HITAC S-820)

	Coil motion parallel to a flaw	Coil motion perpendicular to a flaw
Number of nodes	1373	1278
Number of elements	240	220
Number of nodes on boundary surface	746	716
Number of elements on boundary surface	208	194
Half band width	477	387
CPU time (sec) (500Hz)		
Matrix generation	137	118
Lu *decomposition*	8	6
Back substitution	184.5	86
Flux calculation	62.5	51
Totoal Time	392	261